

APPLICATION OF INFRARED SCANNERS TO

FOREST FIRE DETECTION

Stanley N. Hirsch, Project Leader

U.S. Department of Agriculture, Forest Service
Intermountain Forest and Range Experiment Station
Northern Forest Fire Laboratory
Missoula, Montana

Stanley N. Hirsch received his B.S. degree in electronic engineering at the University of New Mexico and has done graduate work at the University of Idaho. Prior to joining the Forest Service in 1961, Mr. Hirsch served as Senior Instrumentation Engineer for Sandia Corporation and General Electric Company.

As Project Leader for Project Fire Scan, Mr. Hirsch has received international recognition for his work in remote detection of heat sources obscured by smoke and timber cover. His involvement in the development of airborne electronic fire surveillance systems led to a fire mapping system which became operational in the USDA Forest Service's Division of Fire Control in 1966. The unique bispectral IR fire detection system, developed under his leadership, was successfully tested in 1970 and will become operational within the Forest Service in 1971. Mr. Hirsch has served as a member of the forestry committee of NASA's remote sensing group and also in an advisory capacity to the remote sensing project at Pacific Southwest Forest and Range Experiment Station, Berkeley, California.

APPLICATION OF INFRARED SCANNERS TO
FOREST FIRE DETECTION

Stanley N. Hirsch^{1/}

Forest fires frequently spread slowly immediately after ignition. During this period they are easily suppressed. The function of a detection system is to find fires before they grow large enough to cause serious suppression difficulty. Outputs of smoke and radiant energy, which are the key characteristics in forest fire detection, are extremely variable. During the time from ignition until a fire has grown to a size where it is difficult to control, the radiant energy and the smoke outputs may increase continuously with time. More commonly, however, there is a high initial output of either smoke or flame or both smoke and flame, followed by long dormant periods interrupted occasionally by bursts of flame and/or puffs of smoke. Outputs of both smoke and heat usually decrease significantly at night. We have not been able to find any direct correlation between outputs of smoke and radiant energy (Fig. 1).

All forest fire detection systems now being used rely upon visual observation of smoke from lookout towers or aircraft. Such systems are only efficient during daylight hours when a column of smoke is well developed and rises above the trees and when the atmosphere is clear, not contaminated.

Because of these limitations, our project began to investigate the potential of infrared (IR) detection systems. We recognized that an IR device could not be operated from lookout towers because rough topography and heavy timber severely limit the probability of obtaining an unobscured line of sight to ground fires burning under a timber canopy. A direct "look" is needed because reliable detection cannot be achieved from the small amount of radiant energy produced by smoke columns rising above a fire. Therefore, we proceeded with a study of the IR detection probability from aircraft.

At the outset of our studies, we did not know the probability of having an unobscured line of sight between an aircraft and a fire burning under a timber canopy (Fig. 2). We suspected it was strongly dependent on timber characteristics (stand height, bole diameter, number of stems per acre, live crown ratio, and crown characteristics) as well as angle of view and fire size. Therefore, we conducted rather extensive tests in 1963-65 in timber

^{1/} Author is Project Leader for Project Fire Scan, USDA Forest Service, Intermountain Forest and Range Experiment Station, Ogden, Utah; stationed at the Northern Forest Fire Laboratory, Missoula, Montana.

types representative of stands found on the North American Continent [1],[2],[3],[4]. Initially, we conducted flight tests; later we added a mountaintop test because the cost of obtaining sufficient data using aircraft would have been prohibitive. We found that reliable detection for simulated fires of 5 square feet^{2/} could be achieved at angles up to 60° from the nadir (as shown in Fig. 3).

An IR system scanning 120° at 15,000 feet at ground speeds in excess of 200 knots could economically compete with an airborne visual detection system which costs approximately 6¢ per square mile. From 15,000 feet, a 2-milliradian (mrd) resolution system has a ground resolution of 30X30 feet directly under the aircraft and 60X120 feet at 60° from the nadir. This provides enough terrain detail to determine target location. Fire targets of the size we must detect (1 to 10 square feet) will occupy between 1.4×10^{-4} to 1.1×10^{-2} of the instantaneous field of view, depending on the angle of observation and size of the fire. The effective target size may be further reduced because of obscuration by timber. Many of the targets detected in the mountaintop tests were up to 95 percent obscured.

The radiant energy from a forest fire (600°C) peaks in the 3- to 6- μ (micron) region.^{3/} We obtained a 2-mrd IR line scanner with about 1/2° temperature sensitivity (InSb) and began to evaluate its performance. After 2 years of flight testing we found that many of the fires we detected produced very marginal targets. If an interpreter knew the target locations he was usually able to detect them, but the signatures produced on the imagery were so marginal that randomly located targets in a large search area were not detectable.

If a 600°C target fills less than 2×10^{-2} field of view of the scanner, the target's signal-to-background ratio in the 3- to 6- μ region is insufficient to distinguish fire targets from background

^{2/} The probability of detecting a fire of any size may be inferred by assuming that the probability of detecting a fire with 5-ft.² of burning material is equal to the probability of seeing at least one of five 1-ft.² fires. To extrapolate the data in figure 3 to fires of smaller or larger areas, the following may be used:

$$P_n = 1 - (1 - P_5)^{n/5}$$

where:

n = area of fire in ft.².

^{3/} μ = 1×10^{-6} meters.

thermal anomalies. In the 8- to 14- μ region, the target's signal-to-background ratio is less than it is in the 3- to 6- μ region. We began to wonder if we could use the 3- to 6- μ and 8- to 14- μ regions in combination to enhance the target.

Figure 4 shows the 3- to 4- μ (A) and 8.5- to 11- μ (B) signals from both terrain background and fire targets as seen by a 2-mrd system from 15,000 feet plotted in two-dimensional vector space [5]. The lower curve contains all background temperatures from 0° to 60°C.^{4/} The set of points above (shaded area) contains target signatures from fires ranging in temperatures from 600° to 800°C, areas ranging from 1 to 10 square feet, angles of view from 0° to 60°, and obscuration ranging from 0 to 95 percent. Amplitude discrimination in the A channel (horizontal line) would not provide effective separation of targets from background, nor would amplitude discrimination in the B channel (vertical line).

A sloping, straight line drawn between the lower curve and the target points does provide discrimination for most targets. The equation of that line is:

$$A = KB + C$$

where:

$$A = \int_3^4 W_\lambda T_A T_{FA} R_{DA} d\lambda$$

$$B = \int_{8.5}^{11} W_\lambda T_A T_{FB} R_{DB} d\lambda$$

K = slope of discrimination line

C = displacement from origin

W_λ = Planck function

T_A = transmission of atmosphere

T_{FA} = transmission of A channel filter

T_{FB} = transmission of B channel filter

R_{DA} = responsivity of A channel detector

R_{DB} = responsivity of B channel detector

^{4/} Variations in spectral emissivity will spread the background points forming a band rather than the discrete curve shown in figure 4.

or, rewriting and redefining K:

$$K'A - B - C = 0$$

If the background temperature range can be predicted for a given flight, an optimum K can be selected. An effective decision rule and one that is easy to implement in an analog system is: A target exists if the signal is greater than $KA - B$. A nonlinear function that more closely matched the lower curve would be an even more efficient rule, but it would be more difficult to implement. We employed the $KA - B$ function and found it quite effective.

To minimize the effects of changes in atmospheric moisture, we selected the 3- to 4- μ and 8.5- to 11- μ bands rather than the total 3- to 6- μ and 8- to 14- μ windows. We empirically selected spectral regions centered around 3 μ and 8 μ , where the ratio of the power is relatively insensitive to changes in atmospheric moisture.

The way we implemented the bispectral system is shown in figure 5. The 8.5- to 11- μ channel produces high quality infrared imagery from which the position of targets can be accurately determined with respect to terrain features.

The $KA - B$ signal is pulse-height/pulse-width discriminated. A pulse above a preset threshold and within the pulse-width^{5/} limits produces a logic pulse that is stored in a digital memory for one scan line. If a logic pulse is produced at the same point in two successive scan lines, an output pulse is generated. To eliminate false alarms caused by electrical noise, sufficient overscan is available to permit scan-to-scan comparison. The output pulse produces a mark on the edge of the film and reinserts a pulse in the video, which cues the operator (Figs. 6 and 7).

The curvature of the function shown in figure 8 permits selection of two temperatures where the signal amplitude is equal. To calibrate the system we select a pair of temperatures that will produce equal signals in the difference channel for the desired K value. We set the internal calibration sources at these temperatures,^{6/} and then adjust the gain of the 8.5- to 11- μ

^{5/} Pulse-width limit is set to equal the dwell time for one resolution element.

^{6/} Atmospheric transmission is not included in the integration for A and B in figure 8 since the path between the detector and calibration sources is short.

channel until the signal from the two sources is equal. This simple procedure assures that the ratio of total gain (amplifier, detector, and optics) in both channels is optimum for differentiating between targets and any preselected background range.

We calculated the performance of both the single and bispectral systems and predicted that the bispectral system could produce a 12:1 improvement in detecting 1-ft.², 600°C targets against backgrounds ranging from 0° to 50°C. To check our calculations we performed flight tests using thermal anomalies in Yellowstone National Park to provide a high contrast background. The results of these tests showed a 10:1 improvement.

The test was performed in April 1970 when nighttime surface temperatures were -10°C in areas unaffected by geothermal activity. As shown in figure 9, the temperature at Fire Hole River was 10°C, and that for Hot Lake, which is located adjacent to a geyser, was 50°C. Buckets of glowing charcoal were used as targets with surface areas of 1/2, 1, and 2 ft.².

We overflew the area at 15,000 feet above terrain. In addition to the normal film recording and TDM marks, we recorded the 3- to 4- μ , 8.5- to 11- μ , and KA - B signals on magnetic tape. After the flight we photographed the video signals from the tape recordings.

The signals from the 1/2- and 1-ft.² targets were easily differentiated from signals for Hot Lake in the KA - B channel. The signal from the 1-ft.² target was slightly larger than the signal from Hot Lake in the 3- to 4- μ channel. None of the targets produced measurable signals in the 8.5- to 11- μ channel.

During July and August of 1970, the equipment was operationally tested in an 8,000-square-mile area adjacent to Missoula, Montana. On 42 patrol flights, of 5-1/2 hours' duration each, over 800 hot targets were detected and plotted. More than 200 of the targets were wildfires. Forty-five of these were detected by the IR system before they were detected by the presently used visual system of 59 lookout towers and seven patrol aircraft (Fig. 10).

Many fires were detected visually but missed by the IR system, and many fires were detected by the IR system but missed visually. Until we learn more about the relationship between heat output and smoke output from latent fires we cannot determine the relative effectiveness of visual and IR systems. The results of the 1970 tests convinced us that IR used in combination with

visual detection will result in a more efficient system than visual alone. Even with our limited knowledge of the relative effectiveness of the two systems we can begin operational use of a combined system and substantially reduce total firefighting costs (detection plus suppression) [6]. The ultimate potential will not be realized until we are able to arrive at optimal combinations.

REFERENCES

- [1] S. N. Hirsch, "Applications of remote sensing to forest fire detection and suppression," 1962 Proc. Second Symp. Remote Sensing Environ., pp. 295-308, illus., 1963.
- [2] _____, "Preliminary experimental results with infrared line scanners for forest fire surveillance," 1964 Proc. Third Symp. Remote Sensing Environ., pp. 623-648, illus., 1965.
- [3] _____, "Project Fire Scan--summary of 5 years' progress in airborne infrared fire detection," 1968 Proc. Fifth Symp. Remote Sensing Environ., pp. 447-457, illus., 1968.
- [4] R. A. Wilson, "Fire detection feasibility tests and system development," 1968 Proc. Fifth Symp. Remote Sensing Environ., pp. 465-477, illus., 1968.
- [5] Committee on Remote Sensing for Agricultural Purposes, "Remote sensing (with special reference to agriculture and forestry)," Wash., D.C.: Nat. Acad. Sci., pp. 360-410, 1970.
- [6] P. H. Kourtz, "A cost-effectiveness analysis of a simulated airborne infrared forest fire detection system," Ph.D. dissertation, Univ. of California, Berkeley, 1970.



A



B

Fig. 1. These two photographs point up the role that smoke and radiant energy play in the development of forest fire detection systems. A, Flames indicate a high output of radiant energy. In such instances this fire could be readily detected by an IR system, but not by a visual system. B, The output of radiant energy from the fire is too small to enable detection by an IR system, but the well-developed smoke column would be readily detected by a visual system.



Fig. 2. This photograph of the western white pine stand used in the tests shows the "obscuring" effect of a typical forested area.

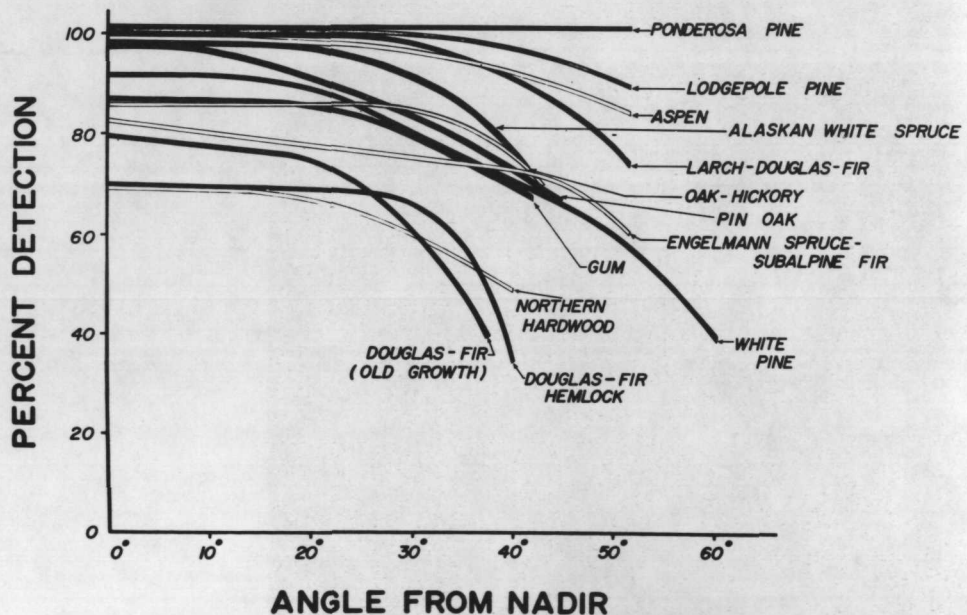


Fig. 3. Shown here are detection probability curves for the 13 timber types tested. Target arrays were five 1-ft.² buckets of glowing charcoal placed on the circumference of a 9-ft. circle. Flight passes were flown at 10° angular increments from 0° to 60° from the nadir.

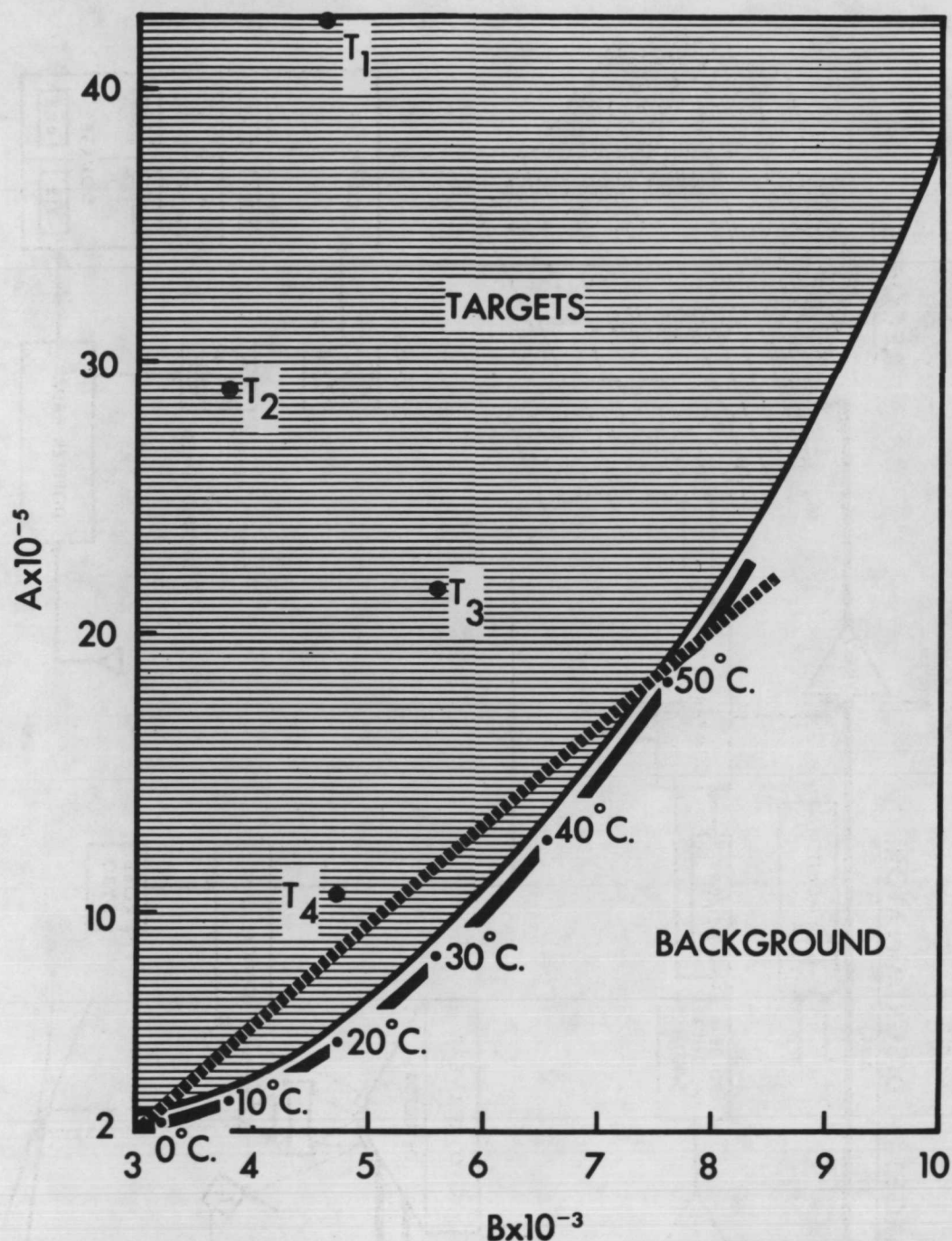


Fig. 4. The signals for both **targets** and **background**, as seen by the 2-mrd IR detection system from 15,000 feet, are plotted in two-dimensional vector space, where A is the 3- to 4- μ and B is the 8.5- to 11- μ vector. Annotation of the target and background temperatures, areas, and angles of view for detected targets is as follows: $T_1=1 \text{ ft}^2$, 600°C, 20° background, 0° angle; $T_2=1 \text{ ft}^2$, 600°C, 10° background, 30° angle; $T_3=1 \text{ ft}^2$, 800°C, 30° background, 60° angle; and $T_4=1 \text{ ft}^2$, 600°C, 20° background, 60° angle.

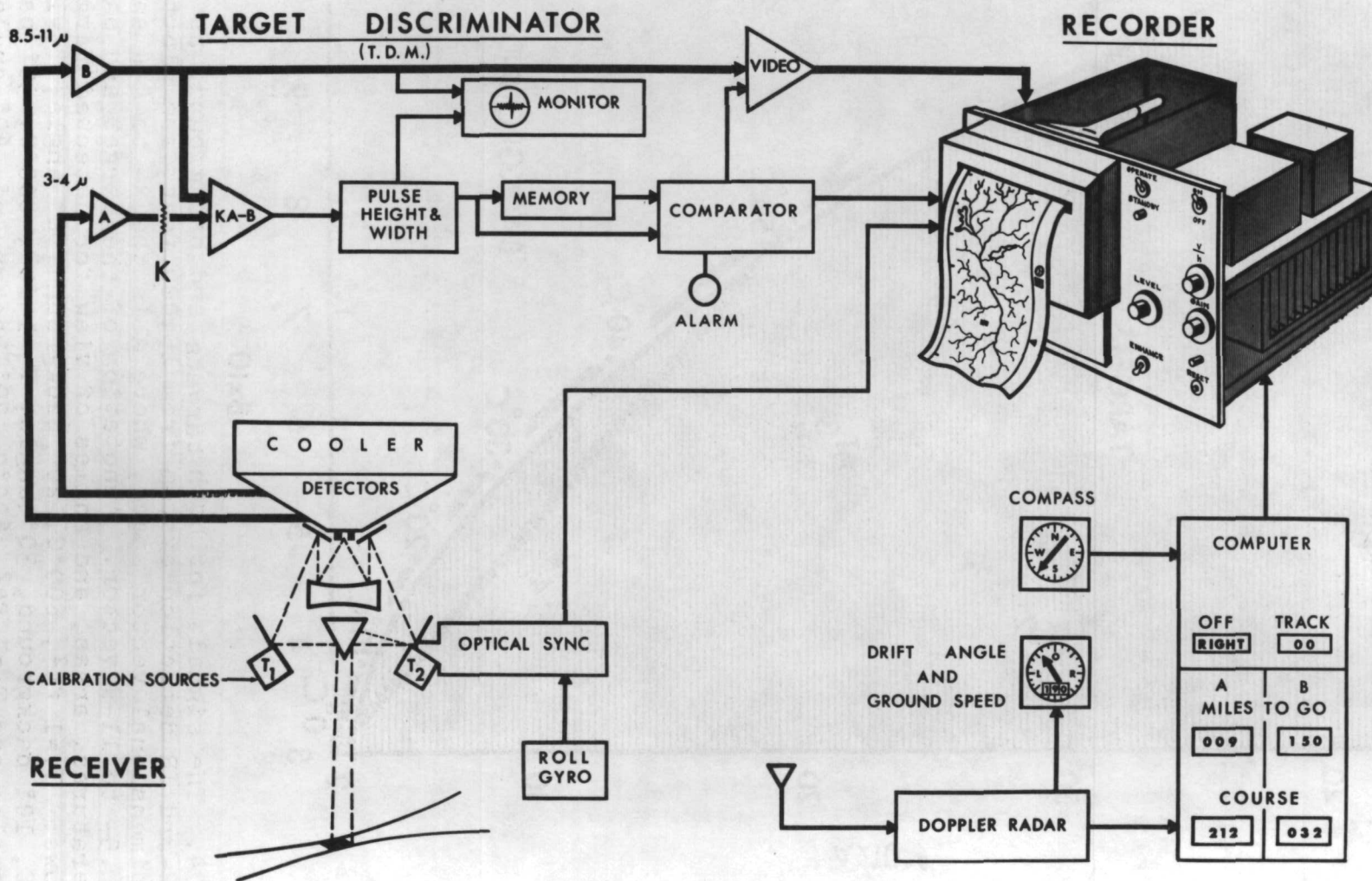


Fig. 5. Shown is a block diagram of the bispectral IR fire detection system.



Fig. 6. The IR fire detection system is designed for operation in a twin turbo-prop, light executive, pressurized aircraft.



Fig. 7. A, Looking forward, the scanner control console, which uses 5-inch film (left foreground) that is processed in near real time.



Fig. 7. B, The special equipment for the IR fire detection system required a modification of the fuselage by the factory. Looking aft, scanner mounted in specially constructed hatch. When closed, the cover for the hatch forms a pressure seal. Helium refrigerator shown provides detector cooling.

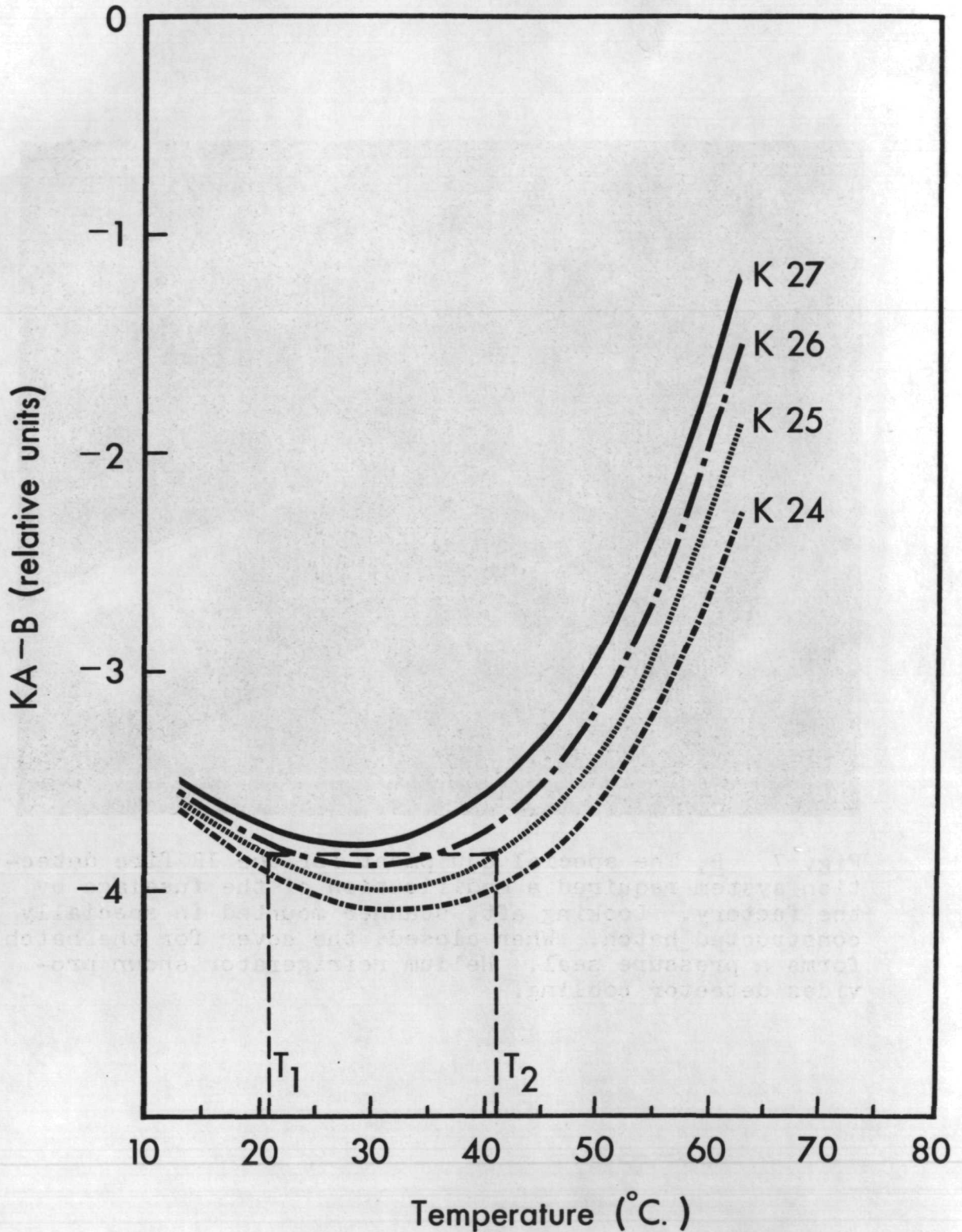


Fig. 8. Shown here is the KA - B signal plotted against temperatures for several values of K. To calibrate the system, T_1 and T_2 are selected to produce equal signals in the difference channel for the desired K value.

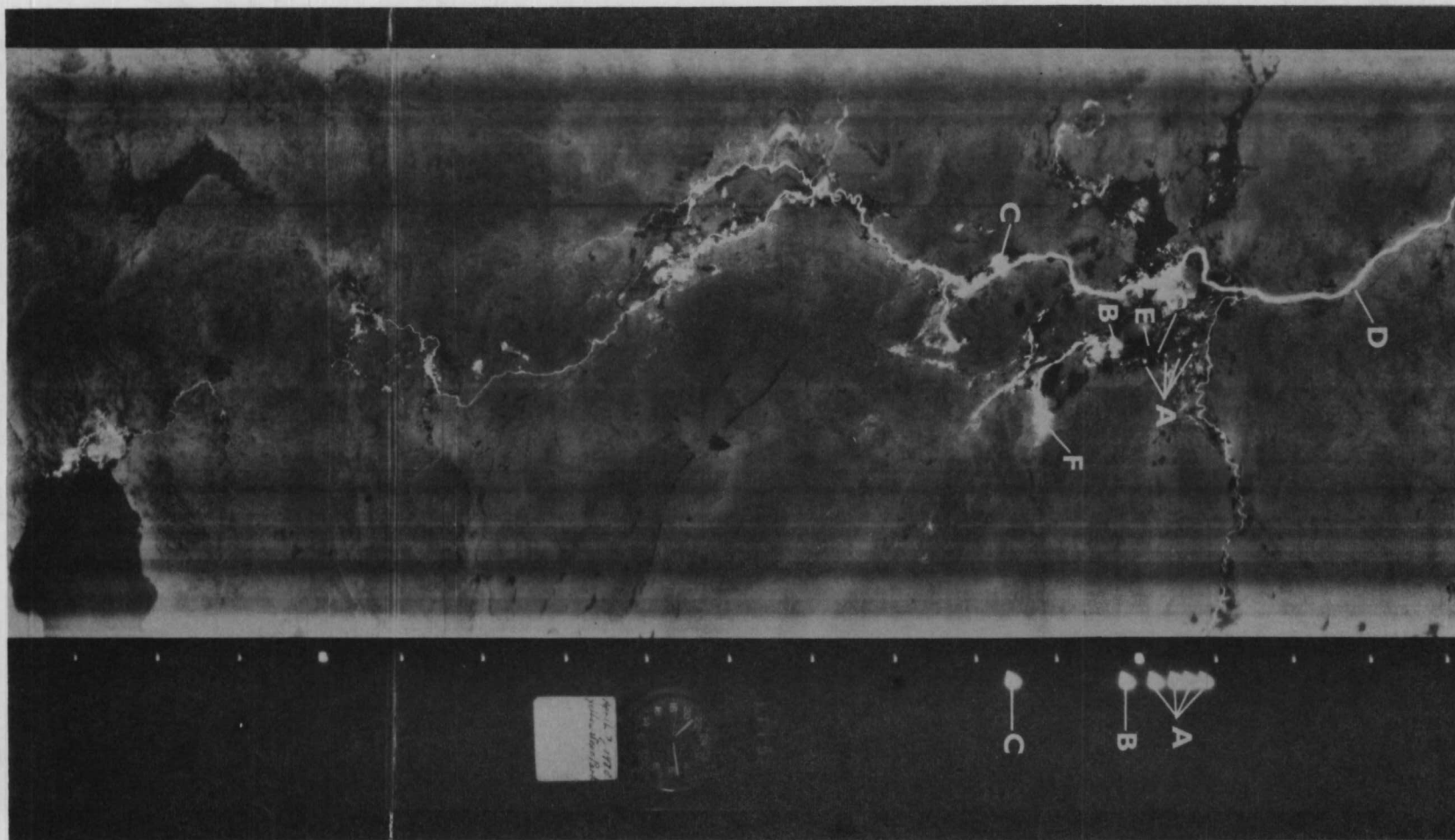


Fig. 9. Shown here is imagery from the test flight over Yellowstone National Park on April 7, 1970, at 2115 hours, and is annotated as follows: A, Trips on test targets (600°C); B, Kaleidoscope Geyser; C, Excelsior Geyser; D, Fire Hole River (10°C); E, snowfield (-13.6°C); F, Hot Lake (52°C); and G, asphalt road (-9°C).



A



B



Fig. 10. This lightning-caused, latent or incipient-type fire (A) occurring in one tree in this area (B) was first spotted in this imagery (C) which was recorded at 0005 hours on July 16, 1970, in an aircraft flying at 21,000 feet. The fire was still burning when photo B was taken. The imagery is annotated as follows: (1) Target is a campfire at Twin Lakes; (2) TDM marks (double marks at the latent fire are due to aircraft pitching during the run); (3) actual fire; and (4) navigation marks at 1-mile intervals.